Nuclear Hyperfine Populations for D Atoms Generated by the 266 nm Photolysis of DI†

Michael Johnson, Lucinda Pringle, Xiaodong Zhang, K. Thomas Lorenz, and Brent Koplitz*

Department of Chemistry, Tulane University, New Orleans, Louisiana 70118

Received: January 8, 2003; In Final Form: April 16, 2003

Results are presented on the photolysis of DI at 266 nm. An experimental approach is used that combines narrow-band, velocity-aligned Doppler spectroscopy (VADS) and a constrained detection geometry. Atomic deuterium is detected, and transitions out of the individual nuclear hyperfine states of the ground electronic state (the *F* states; 0.010 92 cm^{-1} splitting) are resolved via the Lyman-α transition (∼82 280 cm^{-1}). Consistent with previous work on the hydrogen halides, the D-atom product state distributions are statistical. However, the methodological improvements required to resolve the states bode well for studying other chemical systems with this approach.

I. Introduction

Product state distributions resulting from reactions provide insight into the chemical pathways that generate them. Laser-based photodissociation reactions have been yielding such insight for the last several decades.[1] In recent years, a research focus in our group has been on the investigation of the simplest product state distribution, namely, the *F* states that comprise the ground electronic state of atomic hydrogen.[2−4] Brought about by the interaction of the nuclear and the electron spins (each $^1/_2$), the separation in energy between the states (0.0474 cm^{-1}) gives rise to the famous 21-cm line. This 21-cm transition from $F = 1$ to $F = 0$ in atomic hydrogen is important in many studies, including those in astrophysics. Our investigations, while challenging experimentally, have been restricted to more earth-bound studies that involve nuclear hyperfine populations when the photolysis target is HBr, HI, or H_2Se.[2−4]

Central to these experiments is the method known as velocity-aligned Doppler spectroscopy (VADS). Pioneered by Wittig and co-workers,[5,6] the technique relies on temporal and spatial constraints to interrogate selected product velocity vectors.[7−11] Instead of conducting a photolysis/probe experiment that measures all velocity projections on the probe axis, one can delay the two lasers so that only those photoproducts traveling forward or backward along the probe axis are sampled. The resolving power of the VADS method was enhanced significantly in the mid-1990s when it was recognized that one could separate the photolysis and probe laser beams spatially and still achieve good signal-to-noise.[2,3] By sacrifice of one-half of the Doppler profile, use of a ring laser as a probe, and use of a supersonic expansion to cool the parent molecules, resolution was improved by an order of magnitude. Moreover, it was shown that the nuclear hyperfine states of the H atom could be probed for the first time as the result of a chemical reaction.

In the current work, we report on results in which the product is the D atom and the interrogating photon energy is ∼82 280 cm^{-1}. In contrast to the H atom, the nuclear spin is 1 for the D atom, so the *F* states are identified as $^3/_2$ and $^1/_2$. Furthermore, the nuclear hyperfine spacing is 0.010 92 cm^{-1},[12] so one needs to increase the experimental resolving power by a factor of 5 to achieve results comparable to the H atom. As is the case for the H atom in hydrogen halide photolysis,[2,3] the *F* state populations for the D atom are essentially statistical. However, the experimental strategies used to resolve the *F* states for the D atom are important, and a discussion of these strategies, as well as the implications for other experiments, is provided.

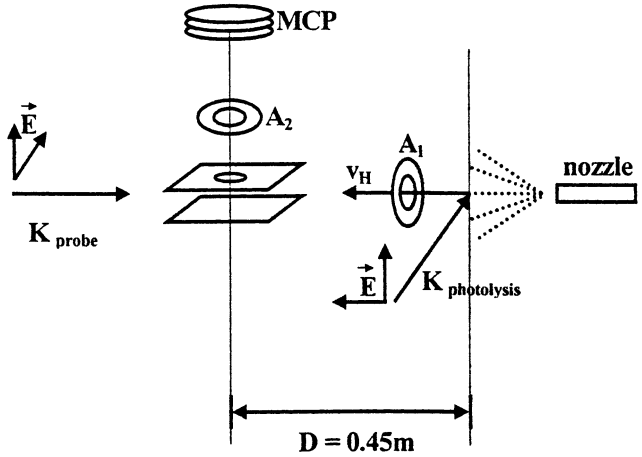

Figure 1. Schematic diagram of the experimental apparatus. A_1 and A_2 denote adjustable apertures. MCP is the microchannel plate detector. The laser beams are shown here in the T-configuration, that is, perpendicular to each other.

II. Experimental Section

Previous versions of the evolving experimental setup have been described elsewhere.[2−4] To recap, neat HI or DI is introduced into the vacuum chamber through a commercially available pulsed nozzle (General Valve series 9; backing pressure ≈ 3−4 atm). The target molecule is photolyzed with the focused output (25 cm focal length lens) of the fourth harmonic of a Nd:YAG laser (Coherent Infinity; <0.1 cm^{-1} bandwidth at 266 nm; 3 ns; ∼20 mJ). The basic experimental configuration is shown schematically in Figure 1. The molecular expansion is intersected by the photolysis beam 4 cm from the nozzle orifice. A portion of the recoiling hydrogen or deuterium atom packet travels 0.45 m into the ionization region of a time-of-flight (TOF) mass spectrometer (R. M. Jordan Co.), where

† Part of the special issue "A. C. Albrecht Memorial Issue".
* Corresponding author.

10.1021/jp0300086 CCC: $25.00
Published on Web 05/24/2003

it is intersected after an appropriate delay by the probe laser beam. For most of the studies in this work, the probe beam is aligned antiparallel to the average velocity vector of the atom packet and perpendicular to the photolysis beam. We term this geometry the T-configuration. For illustration, one spectrum is presented (Figure 3) for which the probe beam was aligned parallel to the photolysis beam and perpendicular to the atom packet. This geometry is called the H-configuration.

The product states are interrogated through $1 + 1'$ (121.6 + 365 nm) resonance-enhanced ionization through the Lyman-α transition. The probe laser consists of the output of an Ar^+-pumped ring laser (Coherent 899-29; Ti:sapphire; 730 nm) seeded into a pulse-amplifier chain. The seed beam is pulse-amplified in two sequential excimer-pumped cuvettes (308 nm pump; rhodamine 700 dye) and then frequency-doubled in a BBO crystal. The resulting 365 nm radiation is then pulse amplified in one final cuvette (308 nm pump; DMQ dye). This laser light (∼12−20 mJ/pulse; 365 nm) is focused into a stainless steel frequency-tripling cell (15 cm length) containing krypton (∼90−150 Torr). This arrangement produces narrow bandwidth (<0.005 cm^{-1}) tunable laser light in the Lyman-α region. The low efficiency of the tripling process means that most of the 365 nm light passes through the system thereby providing the second photon needed in the ionization scheme. The H or D atoms are ionized in an electric field, accelerated, and directed to a high-sensitivity, 40 mm microchannel plate detector at the end of a TOF tube. Spectra are recorded by monitoring the H- or D-atom signal intensity as a function of the probe laser frequency for a given pump−probe laser delay. The product states observed in this study are the nuclear hyperfine states of hydrogen and deuterium.

There are several experimental factors that have been considered in an effort to improve our experimental resolution and to successfully resolve the closely spaced quantum states in this study. First of all, the spectral bandwidth of the probe laser must be sufficiently narrow. A commercially available ring laser provides this capability. Second, the velocity distribution of the parent molecules must be restricted. Cooling can be accomplished with a supersonic jet expansion. The geometry of the experiment must also restrict the effective photolysis and probe volumes. This restriction is accomplished with the use of a two-chamber vacuum system with two variable apertures, effectively spatial filters. These apertures are labeled A_1 and A_2 in Figure 1.

Finally, we note that it is unlikely that collisions are playing a significant role in the overall process. A product D atom that undergoes a collision(s) should slow. Consequently, collisional events will asymmetrically broaden the observed spectral lines in the direction of no Doppler shift. We see no evidence of this slowing. Rather, if a D atom does undergo a meaningful collision(s), the most likely outcome is that we simply do not observe it.

III. Results

The current work uses a further modification to the VADS method to achieve the experimental resolution required to resolve the closely spaced deuterium nuclear hyperfine quantum states. The photolysis of DI (or HI) at 266 nm is used to produce deuterium (or hydrogen) atoms with a substantial amount of kinetic energy. Note that the two spin−orbit states of the I atom produce two distinct D- or H-atom speeds as a result of this dissociation. All spectra shown in this work arise from H or D atoms correlated with ground spin−orbit state I atoms. Also, most of the spectra reported here are doubly red-shifted because

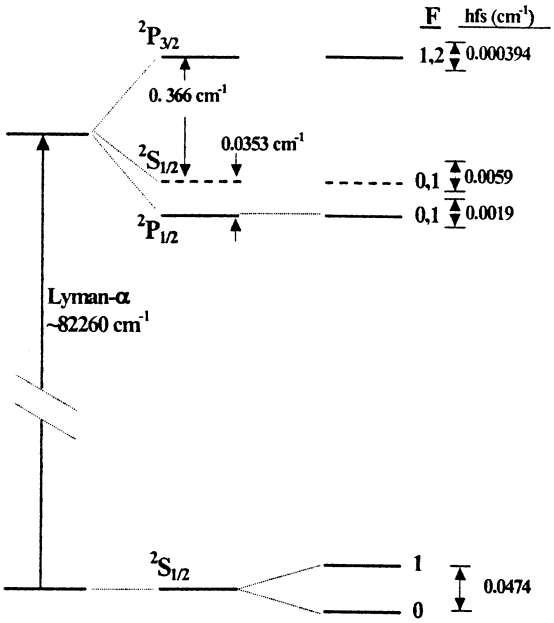

Figure 2. Energy level diagram for the lowest levels of the hydrogen atom. Note that the D-atom nuclear hyperfine splitting is significantly smaller (0.010 92 cm^{-1}) than the H-atom nuclear hyperfine splitting (0.0474 cm^{-1}). However, its Lyman-α transition is actually larger by ∼20 cm^{-1}.

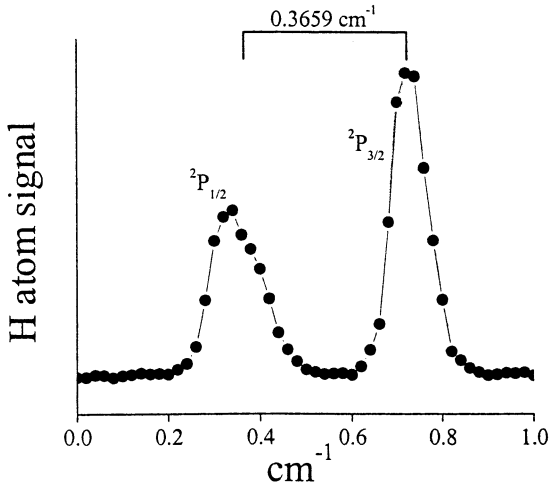

Figure 3. H-atom spectrum taken in the H-configuration. HI was photolyzed at 266 nm, and the laser beams are parallel to one another; thus there is essentially no Doppler shift. The starting point for the scan is 82 268.6 cm^{-1}. The extraction voltage was set to 500 V/cm.

of two contributing effects: the velocity of the parent molecule in the initial jet expansion and the velocity of the H or D atom produced from the kinetic energy disposal that occurs after bond cleavage.

The Lyman-α transition as depicted in Figure 2 is dominated at zero electric field by the $^2S_{1/2} \rightarrow {}^2P_{1/2}$ and $^2S_{1/2} \rightarrow {}^2P_{3/2}$ allowed transitions. Figure 3 shows a low-resolution scan for 266 nm HI photolysis in which little constraint is applied to limit off-axis H-atom velocity components from contributing to the Doppler profile. The spectrum was taken in the H-configuration, thus there is essentially no Doppler shift in the spectrum because the probe beam is perpendicular to the H-atom flight path. Here, the effective photolysis and probe volumes are large enough such that the closely spaced nuclear hyperfine states of atomic hydrogen are not resolved. The shoulder on the $^2P_{1/2}$ peak is due to Stark mixing arising from the applied

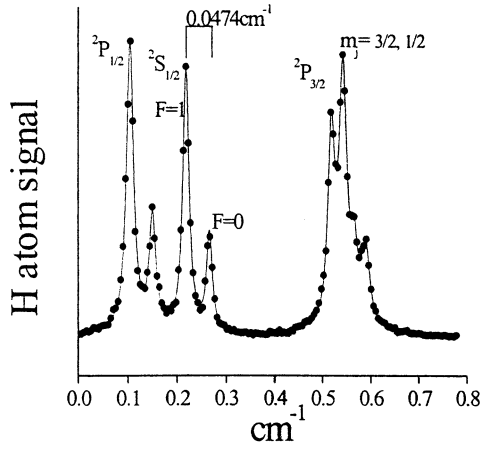

Figure 4. H-atom spectrum taken in the T-configuration. HI was photolyzed at 266 nm, and the laser beams are perpendicular to one another; thus there is a significant red shift to the resonance. The starting point for the scan is 82 253.9 cm^{-1}. The extraction voltage was set to 1000 V/cm. Note that one can identify eight different transitions in the Lyman-α spectrum.

500 V/cm external electric field used to direct the H ions to the MCP. Note that the forbidden $^2S_{1/2} \rightarrow {}^2S_{1/2}$ transition is partially allowed as the 2S $^2S_{1/2}$ state gains P character.

In Figure 4, a greater degree of spatial constraint is applied to the nascent H atoms by using the T-configuration. The applied electric field is raised to 1000 V. The reason for increasing the extraction voltage is to further separate the $^2P_{1/2}$ and $^2S_{1/2}$ states through Stark mixing and to separate the two nondegenerate m_J states of the $^2P_{3/2}$ atomic state.[3] It is seen that there are now four doublets in Figure 4. Each of these doublets results from excitation out of the $F = 0,1$ nuclear hyperfine states of the ground $^2S_{1/2}$ state (see Figure 2). From the relative peak intensities, one can see that the statistical result of 3:1 for the nuclear hyperfine populations is observed for each doublet. While an electric field strength of 1000 V/cm is not quite enough to totally resolve transitions through the individual m_J states, they can be adequately simulated to yield peak areas.

Figure 5 presents a D-atom Doppler scan of the 266 nm photolysis of DI. The two ground $^2S_{1/2}$ nuclear hyperfine states, $F = {}^1/_2$ and $F = {}^3/_2$, are the only populated product states of the D-atom fragment. The energy spacing between these two levels is 0.010 92 cm^{-1},[12] and the extraction voltage has been raised to 1350 V/cm to better resolve the m_J levels in the $^2P_{3/2}$ state. Note that this scan was taken with the pulsed nozzle pointed in the direction of the detection region, so the spectrum is now "doubly" red-shifted. For this spectrum, the interchamber aperture (A_1) was set to its smallest possible size, ~1.5 mm. The detection aperture (A_2) was also set to its minimum, ~0.7 mm. This scan is the result of 100 laser pulses averaged per data point. All of the nuclear hyperfine doublets are sufficiently resolved to simulate, and Lorentzian line shapes were assumed. For clarity, one of the doublets is expanded to reveal the degree of experimental resolution. In the expanded spectrum, the simulated nuclear hyperfine peaks are represented as dots and dashes, while the sum of the two peaks is the bold solid line. Clearly, the fit is good. Note that the ratio used for the F state populations ($^3/_2$:$^1/_2$) is exactly 2.0 to 1.0, the statistical result. Likewise, a 2.0 to 1.0 ratio is observed when the transition involving the $^2P_{1/2}$ state is simulated (not shown).

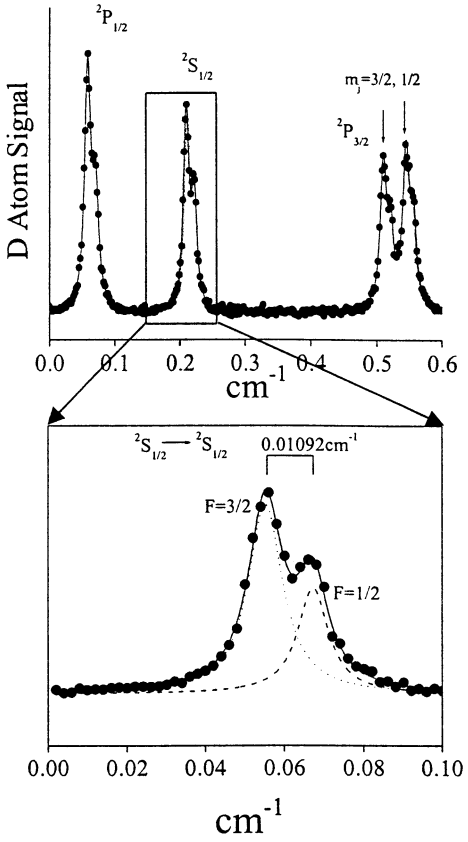

Figure 5. D-atom spectrum taken in the T-configuration. DI was photolyzed at 266 nm, and the laser beams are perpendicular to one another; thus there is a significant red shift to the resonance. In the upper trace, the starting point for the scan is 82 277.64 cm^{-1}. The extraction voltage was set to 1350 V/cm. The expanded spectrum shows a simulation for the transition to the $^2S_{1/2}$ mixed state using a statistical distribution for the nuclear hyperfine F states. Here, the starting point for the scan is 82 277.78 cm^{-1}.

IV. Discussion

Generally speaking, hyperfine interactions have been studied in larger systems. For examples, see ref 13 and references contained therein. In our work, the focus is on H and D atoms, and the discussion is divided into three separate parts. Initially, we address the experimental method, specifically those experimental improvements that are important for increasing spectral resolution. Next, the current results are discussed. Finally, a prognosis for future studies with this method is put forth.

A. Approach. Several experimental factors have enabled the resolution in the experiment to be improved when compared to previous nuclear hyperfine determinations for atomic hydrogen.[2,3] One important aspect is the need to constrain the two flight paths with apertures, shown as A_1 and A_2 in Figure 1. Originally, it was thought that the focal regions defined by the two laser beams (photolysis and probe) provided sufficient constraint on the neutral trajectories because of the relatively long flight distance (0.45 m). However, simulations suggested that apertures, both in the neutral flight path (A_1) and the ion flight path (A_2), would provide a necessary additional restriction on the spatial regions from which H atoms can be observed.[14] Subsequently, these apertures did improve the experimental resolution by further limiting the velocity vectors that are ultimately observed.

An additional experimental feature concerns the position of the supersonic nozzle. As depicted in Figure 1, the nozzle direction is parallel to the flight path of the neutral photoproduct, in this case the D atom. Previous efforts in our laboratory had the nozzle direction essentially perpendicular to the flight direction.[2,3] The new position adds a velocity vector to the speed of the D atom, because the parent beam now has a nonzero

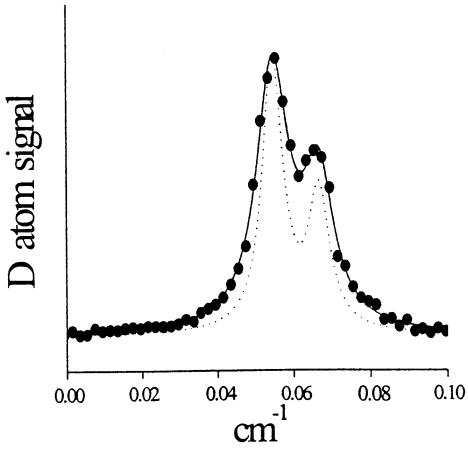

Figure 6. The data from the expanded region of Figure 5 (experimental points) compared with the uncertainty-principle-limited line width. Here, the comparison is made using 0.006 67 cm^{-1} line shapes (see ref 15). The starting point for the scan is 82 277.78 cm^{-1}.

velocity component in the direction of the flight path. However, as long as the molecular beam is translationally cold enough, no significant spectral broadening will be introduced. Only a slight red-shifted spectral offset will manifest itself. On the plus side, velocity vectors perpendicular to the flight direction are reduced. When convoluted with the photolysis focal region, such parent molecule velocity vectors can broaden the observed spectrum.

It should be noted that for the study of D and H atoms detected through Lyman-α with this method, we are nearing a fundamental limitation in the resolution afforded by this approach that is illustrated in Figure 6. Specifically, the uncertainty principle ($\Delta E \Delta t$) places a limit on one's ability to resolve the nuclear hyperfine peaks owing to the spontaneous lifetime of the excited electronic state. Using a line width value of 200 MHz (0.006 67 cm^{-1}),[15] the limiting convolution is shown in Figure 6 in comparison to the observed D-atom experimental line shape. While we are not certain of the spontaneous lifetime for the excited state in the actual electric field used (1350 V/cm), Figure 6 nonetheless shows that a fundamental limitation is being approached.

B. H and D Atom Spectra. From a translational-energy point of view, there are two "types" of H or D atoms that are generated in hydrogen halide photolysis: one correlated with the ground spin−orbit state of the I atom and one correlated with the excited spin−orbit state of the I atom. As previously noted, all spectra presented in this paper are correlated with the ground electronic state of the I atom. Figure 3 provides some experimental perspective. The photolysis and probe laser beams, while separated by 0.45 m, were arranged in the H-configuration, i.e., they were propagating parallel to one another with the H-atom flight path connecting them. Consequently, Figure 3 is essentially a spectrum for the H atom taken with little to no Doppler shift. Two of the major features of the Lyman-α transition are clearly identified, but no nuclear hyperfine resonances can be observed. The presence of the mixed $^2S_{1/2}$ state (now allowed because of the electric field) is seen as a slight shoulder on the transition through the $^2P_{1/2}$ mixed state.

By switching to the experimental T-configuration (shown in Figure 1), reducing the size of the apertures, and using an electric field of 1000 V/cm, one can produce the H-atom spectrum shown in Figure 4. Here, all three excited electronic states of the Lyman-α transition (see Figure 2) are observed, but more importantly, transitions out of the nuclear hyperfine states are readily identified. Moreover, the transition through the $^2P_{3/2}$ state can be broken down into its individual $m_j = {}^3/_2, {}^1/_2$ components. Note that each of these m_J states also contains features originating from the nuclear hyperfine states. Inspection of one of the isolated electronic transitions (e.g., the mixed $^2S_{1/2}$ state) reveals essentially statistical populations, because the expected probability for $F = 1$ to $F = 0$ is 3:1 due to degeneracy considerations.[2]

To our knowledge, Figure 5 presents the first results on the measurement of nascent nuclear hyperfine populations for D atoms generated by a photolysis event, in this case 266 nm DI photodissociation. Consistent with work shown previously[2−4] and above for H atoms, the results are statistical within experimental error. The degeneracies for the D-atom F states ($^3/_2$, $^1/_2$) are different than those for the H-atom F states owing to the different spin on the nucleus. Thus, the statistical result is a 2:1 ratio for peak heights. The expanded part of Figure 5 shows the fit for the mixed $^2S_{1/2}$ state assuming a statistical population for the F states.

While it is experimentally challenging to determine the D-atom and H-atom nuclear hyperfine populations, to date they have been dynamically uninteresting because of the statistical outcomes. Qualitatively, one can think about these statistical results in the following way. The photolysis energy puts the parent molecule well above the dissociation energy. Because the energy spacing is so small in the product states, the H or D atom photoproduct essentially becomes an atom while the dissociating system still has plenty of internal energy. Simple statistics then govern the population of the nuclear hyperfine states.

C. Prognosis. Two general issues are addressed here. The first concerns the nature of nuclear hyperfine populations in H and D atoms. What makes these targets compelling is their simplicity. The wave functions one uses to describe them are exact and can be found in an elementary quantum mechanics textbook.[3] What is needed is a way to make them dynamically interesting, and two approaches come to mind. One way is to use a molecular system that has truly long-range interactions. One such molecule is H_2^+ undergoing dissociation. Here, two protons are moving apart from one another yet constantly interacting with one single electron. The effects of long-range interactions could well manifest themselves in the nuclear hyperfine populations. Moreover, the ability to measure nuclear hyperfine populations for both D and H atoms means that systems such as HD^+ would be possible candidates for study. A second approach for investigation would involve directly affecting the dissociation event with external fields, be they magnetic, electrical, or electromagnetic.

A final issue concerns the applicability of the method to studying systems other than atomic hydrogen. Such experiments are currently underway in our laboratory, and we note that preliminary results are very encouraging for photoproducts such as the Cl atom.

Acknowledgment. One of us (B.K.) is grateful to Professor A. C. Albrecht for unique inspiration at an early stage of his career. We thank the Louisiana Board of Regents, the National Science Foundation, and NASA for support of this work.

References and Notes

(1) El-Sayed, M. A., Ed. *J. Phys. Chem.* **1996**, *100 (*Centennial Issue), 12694−13322. In particular, Butler, L. J.; Neumark, D. M. *J. Phys. Chem.* **1996**, *100*, 12801 and references therein.

(2) Cowen, K. A.; Lorenz, K. T.; Yen, Y.-F.; Herman, M. F.; Koplitz, B. *J. Chem. Phys.* **1995**, *103*, 5864.

(3) Lorenz, K. T.; Cowen, K. A.; Fleming, P. F.; Mathews, M. G.; Herman, M. F.; Koplitz, B. *Chem. Phys. Lett.* **1996**, *261*, 145.

(4) Zhang, X.; Johnson, M.; Lorenz, K. T.; Cowen, K. A.; Koplitz, B. *J. Phys. Chem. A* **2000**, *104*, 10511.
(5) Xu, Z.; Koplitz, B.; Buelow, S.; Baugh, D.; Wittig, C. *Chem. Phys. Lett.* **1986**, *127*, 534.
(6) Koplitz, B.; Xu, Z.; Baugh, D.; Buelow, S.; Häusler, D.; Rice, J.; Reisler, H.; Qian, C. X. W.; Noble, M.; Wittig, C. *Faraday Discuss. Chem. Soc.* **1986**, *82*, 125.
(7) Xu, Z.; Koplitz, B.; Wittig, C. *J. Chem. Phys.* **1987**, *87*, 1062.
(8) Xu, Z.; Koplitz, B.; Wittig, C. *J. Phys. Chem.* **1988**, *92*, 5518.
(9) Xu, Z.; Koplitz, B.; Wittig, C. *J. Chem. Phys.* **1989**, *90*, 2692.
(10) Dixon, R. N.; Nightingale, J.; Western, C. M.; Yang, X. *Chem. Phys. Lett.* **1988**, *151*, 328.
(11) Cromwell, E. F.; Stolow, A.; Vrakking, M. J. J.; Lee, Y. T. *J. Chem. Phys.* **1992**, *97*, 4029.
(12) Prodell, A. G.; Kusch, P. *Phys. Rev.* **1954**, *88*, 184.
(13) Carter, R. T.; Huber, J. R. *Chem. Soc. Rev.* **2000**, *29*, 305.
(14) Zhang, X. Ph.D. Thesis, Tulane University, New Orleans, LA, 2001.
(15) Wild, J. P. *Astrophys. J.* **1952**, *115*, 206.